

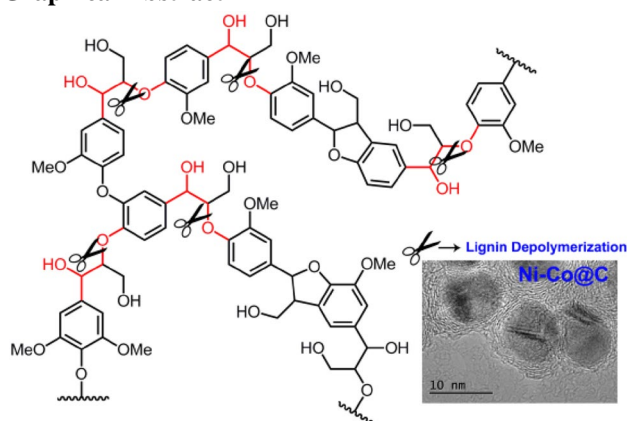
Highly Stable and Recyclable Graphene Layers Protected Nickel–Cobalt Bimetallic Nanoparticles as Tunable Hydrotreating Catalysts for Phenylpropane Linkages in Lignin

Bingfeng Chen¹ · Fengbo Li¹ · Guoqing Yuan¹

Received: 1 April 2017 / Accepted: 25 August 2017
© Springer Science+Business Media, LLC 2017

Abstract Nickel–cobalt bimetallic nanoparticles coated with several layers of graphene were developed through direct heating treatment of bimetallic oxide precursor prepared by the modified Pechini-type sol–gel method. These nanomaterials were demonstrated to be versatile catalysts for lignin depolymerization. The catalysts showed unexpectedly tunable selectivity that directly depends on the composition of bimetallic nanoparticles. Dimeric lignin model compounds can be converted totally and the hydrogenolysis selectivities above 85% over Ni–Co@C (Ni:Co = 1:3). During the recycling test, the nanocatalyst showed excellent recyclability in the ten-batch investigation. The deposition of graphene layers over bimetal nanoparticles fosters a subtle balance between protecting effects and surface accessibility to catalytic reactions and significantly improves their stability to air and moisture. Ni–Co@C catalysts were readily separated from the liquid mixtures with high recycling ratio due to their magnetic properties.

Graphical Abstract



Ni–Co bimetallic nanoparticles are coated with graphene layers. Graphene layers over the nanoparticles protect them from deactivation. Ni–Co@C shows tunable selectivity in the hydrogenolysis of dimeric lignin linkage. The non-precious metal catalyst showed excellent recyclability and can be reused ten times without significant loss of activity.

Keywords Nanoparticles · Bimetallic catalysts · Graphene layers · Hydrogenolysis · Lignin

1 Introduction

Biomass represents an enormous store of renewable carbon resources, which can be used as the feedstocks for the sustainable productions of chemicals and fuels through biorefinery [1, 2]. Lignocellulose materials consist of three primary fractions: hemicellulose (pentose, hexoses), cellulose (glucose-polymer), and lignin (phenol-polymer) [3]. Lignin is plant polymer made from phenylpropanoid building units

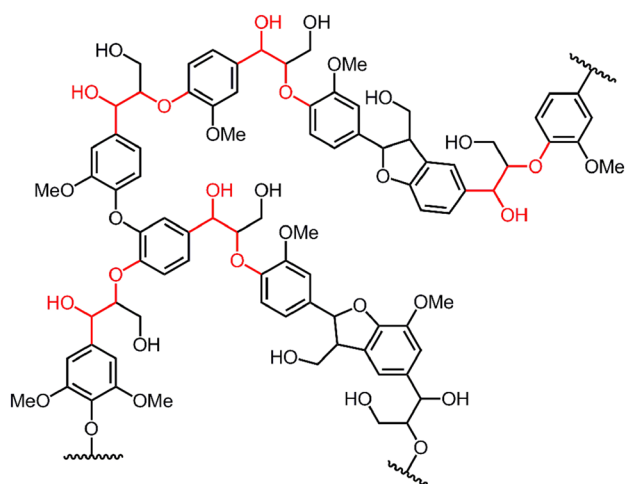
✉ Fengbo Li
lifb@iccas.ac.cn

✉ Guoqing Yuan
yuangq@iccas.ac.cn

¹ Beijing National Laboratory of Molecular Science, Key Laboratory of Green Printing, Institute of Chemistry, Chinese Academy of Sciences, Beijing 100190, People's Republic of China

through a series of characteristics linkages and end groups [4, 5]. These building blocks are connected with each other to produce the complex architecture of lignin. There are several linkages of the monolignol units that form different C–O and C–C intermonomeric bonds in the polymer, as shown in Scheme 1.

Native lignins and separated lignins are the only renewable resource for producing industrial aromatics. Through a well-designed depolymerization process, lignin matrix may be broken into a family of high-value phenolic structures, such as cresols, catechols, resorcinols, quinones, or guaiacols [6]. However, pathways for producing high-value molecules from lignin are in their very early state and the selective transformation of lignin remains a great challenge [7]. There are several potential strategies for lignin depolymerization. Thermochemical processes (combustion, gasification, thermolysis, and hydrothermal hydrolysis) are generally nonselective [8]. Although hydrotreating of lignin leads to the increasing demand for hydrogen, it is one of the most promising methods for depolymerization of lignin, which can produce simple molecule mixtures with high yields. Catalytic cracking of C–O intermonomeric bonds in the presence of hydrogen, generally termed hydrogenolysis, has attracted much attention for lignin valorization. 2-Phenoxy-1-phenylethanol is always serviced as lignin model compound for the β -O-4 linkage, which accounts for approximately 50% of all the linkages in lignin [9]. Ru/CNT was used in the hydrodeoxygenation of lignin-derived phenols in a biphasic H_2O/n -dodecane system [10]. Pd/C was employed as a catalyst for the cleavage of β -O-4 ether bonds in lignin model compounds and moderate depolymerization of native lignins [11, 12]. Supported Pd–Fe bimetallic catalyst has been reported in the catalytic hydrogenolysis of phenethyl phenyl ether into aromatics [13]. Ni–M (M = Au,



Scheme 1 Illustration of lignin fragment with the notation of phenylpropane linkage (carbon–oxygen bond)

Ru, Rh, and Pd) bimetallic nanoparticles catalysts have been reported in the hydrogenolysis of lignin model compounds (β -O-4 linkage) and organosolv lignin [14, 15]. Some catalysts using base metals (Ni, Co, Cu) have been reported in the hydrogenolysis of lignin model compounds. The cracking of β -O-4 lignin-type dimers was catalyzed by Cu/Al_2O_3 or $Cu/MgO-Al_2O_3$ [9]. Supported nickel catalysts, such as Ni/SiO_2 and Ni/TiN , have been used in the hydrogenolysis of aryl ethers as lignin model compounds [16, 17]. Bidy and Beckham also reported that Ni/hydrocalcite was quite active (>99% conversion) in the cleavage of 2-phenoxy-1-phenethanol in methyl isobutyl ketone at 270 °C for 1 h [18]. Recently, $NiAlO_x$ catalyst has been reported in the hydrogenolysis of aromatic ethers to cyclohexanol derivatives in the presence of Lewis acid [19].

Hydrotreating catalysts based on precious metals exhibit efficient catalytic performances. However, their high prices limit the practical application and lead to substantial costs in the required recovery and recycle processes [20–23]. There are great efforts put into developing base metal catalysts (Ni, Co, Cu, Fe) with improved selectivity and recyclability [24, 25]. The quantum size effect of nanoscale materials offers many solutions to develop supported metal nanoparticles and metal species dispersed over nanomaterials. The main drawbacks of base metals (Ni, Co, Cu, Fe) nanoparticles are their instability in air and moisture and fast deactivation under the practical operation [26–28]. In our recent work, carbon-coated Cu–Co bimetallic nanoparticles show excellent catalytic performances in the hydrogenolysis of 5-(hydromethyl)furfural for production of biofuel (2, 5-dimethylfuran) [29].

In this work, a well-designed strategy was developed to prepare nickel, cobalt, and nickel–cobalt mixed nanoparticles, which are coated with several layers of graphene. There is a subtle balance between protecting effects and surface accessibility to catalytic reactions. Carbon-coated nickel–cobalt mixed nanoparticles have unexpectedly tunable selectivity in catalytic hydrotreating of model molecule of phenylpropane linkages in lignin, as shown in Scheme 1. The deposition of graphene layers over the metal nanoparticles markedly improves their stability to air and moisture and leads to excellent recyclability.

2 Experimental

2.1 Catalyst Preparation

Carbon-coated Ni–Co bimetallic nanoparticles were prepared by the modified Pechini-type sol–gel method. $Co(NO_3)_2 \cdot 6H_2O$ and $Ni(NO_3)_2 \cdot 6H_2O$ was added to water (20 ml, total metal amount: 6.25 mmol). The molar ratio of Ni to Co of metal precursors can be adjusted from 3:1

to 1:5. Then tartaric acid (TA, 12.5 mmol) was added to the mixture. Glycerol/water mixture ($v/v = 4:1$, 60 ml) and polyethylene glycol (average MW: 6000, 5.0 g) were added. Nanographite materials (0.5 g) were added and dispersed under sonication for 1.0 h. The mixture was transferred to a hydrothermal reaction vessel, and then heated to 150 °C for 13 h. The solid materials were collected by centrifugal separation, and washed with ethanol for three times, and dried at 100 °C overnight. The carbon-coated Ni–Co bimetallic nanoparticle catalysts were obtained by thermal treatment of the precursors at 800 °C in argon flow for 2 h. The carbon-coated Ni or Co catalyst was prepared by the similar method, and $\text{Ni}(\text{NO}_3)_2 \cdot 6\text{H}_2\text{O}$ or $\text{Co}(\text{NO}_3)_2 \cdot 6\text{H}_2\text{O}$ was used as metal precursor.

2.2 Catalyst Characterization

Powder X-ray diffraction (XRD) patterns were measured on a Rigaku Rotaflex diffractometer equipped with a rotating anode and a Cu-K α radiation source (40 kV, 200 MA; $\lambda = 1.54,056 \text{ \AA}$). Inductive coupling plasma emission spectrometer (ICP-OES) analysis was conducted on the Varian 710 ICP-OES with ICP Expert II software. XPS data were obtained with an ESCALab220i-XL electron spectrometer from VG Scientific using 300 W Al-K α radiations. The base pressure was approximately 3×10^{-9} mbar. The binding energies were referenced to the C1s line at 284.8 eV from adventitious carbon. The Eclipse V2.1 data analysis software supplied by the VG ESCA-Lab200i-XL instrument manufacturer was used to manipulate the acquired spectra. Transmission electron microscopy (TEM) was performed on a JEOL 2010 TEM equipped with an attachment for local energy dispersion analysis (EDX). The accelerating voltage was 200 kV, and the spot size was 1 nm. High-angle annular dark field scanning transmission microscopy (HAADF-STEM) was performed on the carbon-coated Ni–Co bimetallic nanoparticles catalysts with JEOL JEM-2100F microscope in a scanning transmission electron microscopy (STEM) mode operated at 200 kV.

2.3 Catalyst testing

Lignin model molecule (2-phenoxy-1-phenylethanol) was synthesized according to the method reported by Rothenberg [9]. Catalytic hydrotreating of 2-phenoxy-1-phenylethanol was carried out in a 100 ml autoclave with Teflon liner. The catalyst (50 mg) was added to a solution of 2-phenoxy-1-phenylethanol (150 mg) in ethanol (2 ml) and H_2O (8 ml). The autoclave was sealed and purged with H_2 several times. The reaction was performed at 170 °C with 2 MPa hydrogen pressure for 6 h. Then, the reactors were cooled down to room temperature using an ice bath, and the organic products were extracted with ethyl acetate (5 ml \times 2). The organic

products mixtures were analyzed by GC and chlorobenzene was used as an external standard. Identification of main products was based on GC-MS as well as by comparison with authentic samples. The product distribution was shown on the mole basis. In consecutive batch tests, the catalyst was recovered by magnets and washed with EtOH for three times. The catalyst was recycled into the autoclave with the feedstream.

3 Results and Discussions

3.1 Development of Nanocatalysts

Through the modified Pechini-type sol–gel process, the mixed metal oxides are formed and coated with polyethylene glycol. Further heating treatment gradually carbonizes the polymer layers, which serve as the carbon sources for graphene layers. Meanwhile, the carbonized polymers are the reductant for the formation of bimetallic nanoparticles. Transmission electron microscopy (TEM) micrograph showed formation of well-dispersed carbon-coated nickel nanoparticles in the range of 3–10 nm (Fig. 1a–c), and the average particle size is about 6 nm. Carbon-coated Ni–Co bimetallic nanoparticles have larger particle size and their average particle size is about 10 nm (Fig. 1d). The graphene layers over the bimetallic nanoparticles are clearly revealed by HRTEM images (Fig. 1e, f). The thickness of carbon shell is about 2–6 nm. These carbon depositions provide direct protection against oxidation and deactivation and improve their recyclability and recoverability. The energy-dispersive spectroscopy (EDS) measurement is carried out to investigate the elemental composition and the distribution of the element in the bimetallic nanocatalysts. Figure 2a shows the selected particles in the marked areas for elemental mapping analysis. Every nanoparticle contains both Ni and Co, and Ni and Co are uniformly distributed in these particles (Fig. 2b, c). Elemental mapping of carbon overlaps the noise signals from carbon membrane of TEM sample support (Fig. 2d).

X-ray photoelectron spectroscopy (XPS) measurement is carried out to investigate the chemical composition of carbon-coated Ni–Co bimetallic nanoparticles. Ni $2p_{3/2}$ and $2p_{1/2}$ XPS peaks are at the binding energy values of 852.3 and 869.7 eV, respectively (Fig. 3A-a). The single metal sample (Ni@Carbon) prepared by the same method shows similar XPS peaks of Ni 2p. These results indicate that nickel is almost in the zero-valent states. Co 2p XPS peaks show more complex patterns (Fig. 3B-c). There are three typical patterns: zero-valent metal species (Co $2p_{1/2}$ 777.5 eV), cobalt oxide species (Co $2p_{1/2}$ 781.6 eV), and the shakeup satellite signals (785.2 and 801.0 eV). The single metal sample (Co@Carbon) shows the same trend

Fig. 1 TEM image (a) and HRTEM images (b–c) of Ni@C; TEM image (d) and HRTEM images (e–f) of Ni–Co@Carbon (Ni:Co = 1:3)

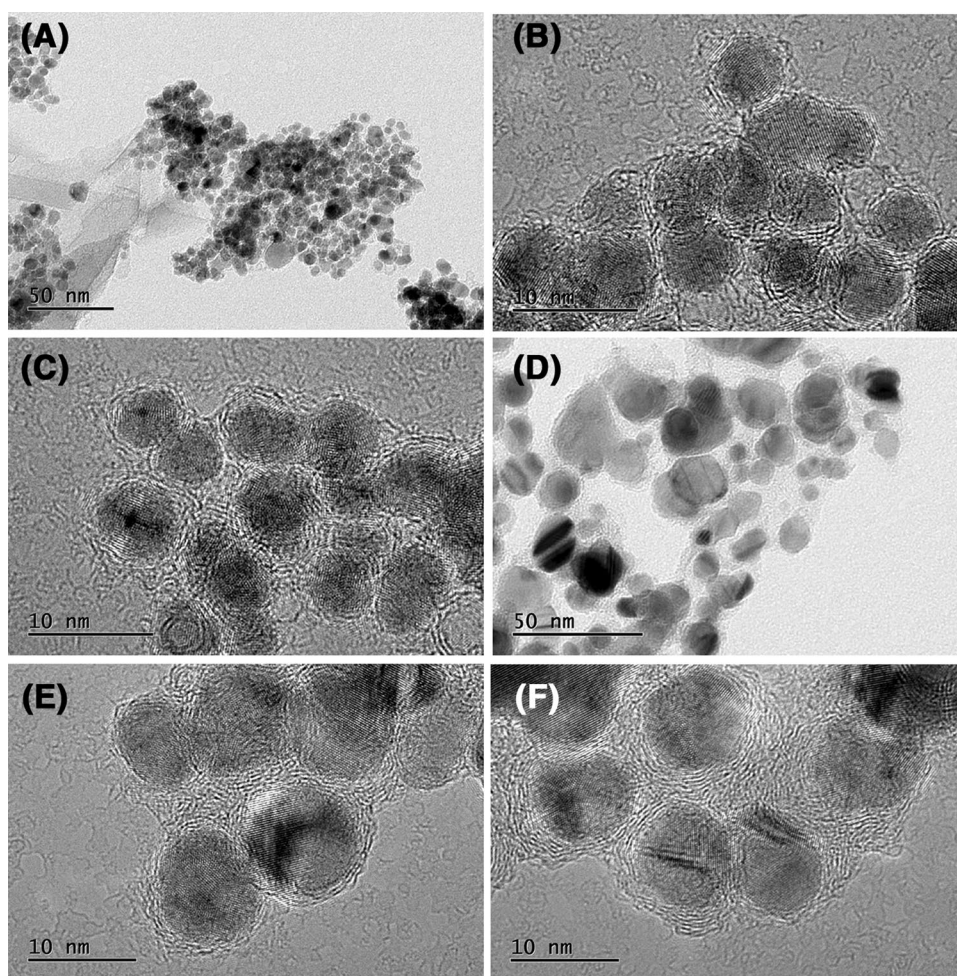


(Fig. 3B–d). However, cobalt oxide species have a higher atomic concentration in the Co@Carbon than that in the Ni–Co@C.

The XRD patterns of monometallic (Ni@C and Co@C) and bimetallic (Ni–Co@C) samples, thermal treated at 800 °C for 2 h under argon atmosphere, are shown in Fig. 4. For Ni@C catalyst, the diffraction peaks located at $2\theta = 44.4$, 51.8 and 76.2° indicated the existence of the characteristics of Ni metal phase (JCPDS 04-0850), while the peaks at 26.4° and 54.5° were assigned to the diffraction of graphite phase (JCPDS 41-1487). For the Co@C catalyst, the diffraction peaks located at 44.2° , 51.5° and 75.9° were ascribed to the characteristics of Co metal phase (JCPDS 15-0806).

3.2 Catalytic Performances in Hydrotreating of Lignin Model Linkages

2-Phenoxy-1-phenylethanol (**1**) in Scheme 2 is selected as the model molecule of the linkage unit in Scheme 1. There are three possible reaction routes: hydrodeoxygenation, cleavage of ether bond, and hydrogenation. To achieve valuable target products, the reaction path should be controlled

through development of catalytic surface with tunable selectivity. Carbon-coated Ni–Co mixed nanoparticles shows unexpected versatility and flexibility in the selectively hydrotreating the lignin linkage unit. Nine products are detected in the final reaction mixtures. Product (**2**) is formed by direct hydrodeoxygenation of the side hydroxyl group. Aryl ether is kept constant and this conversion cannot lead to depolymerization of lignin matrix. Other products are from ether bond cleavage and further hydrodeoxygenation and hydrogenation, which are summed as hydrogenolysis products. Generally, the catalytic cleavage of β -O-4 ether bonds in lignin model compounds is easier than the hydrogenolysis of aryl ether. Benzene has not been detected in the product mixture. The reaction network is shown in Scheme 2.

Table 1 summarizes the results of screening experiments. There is a marked difference in the catalytic performances between carbon-coated nickel and carbon-coated cobalt nanoparticles. The conversion over cobalt monometallic nanoparticles only leads to the hydrodeoxygenation of side hydroxyl group and no cleavage of ether bond is detected (Entry 7 in Table 1). In contrast, the products of ether bond

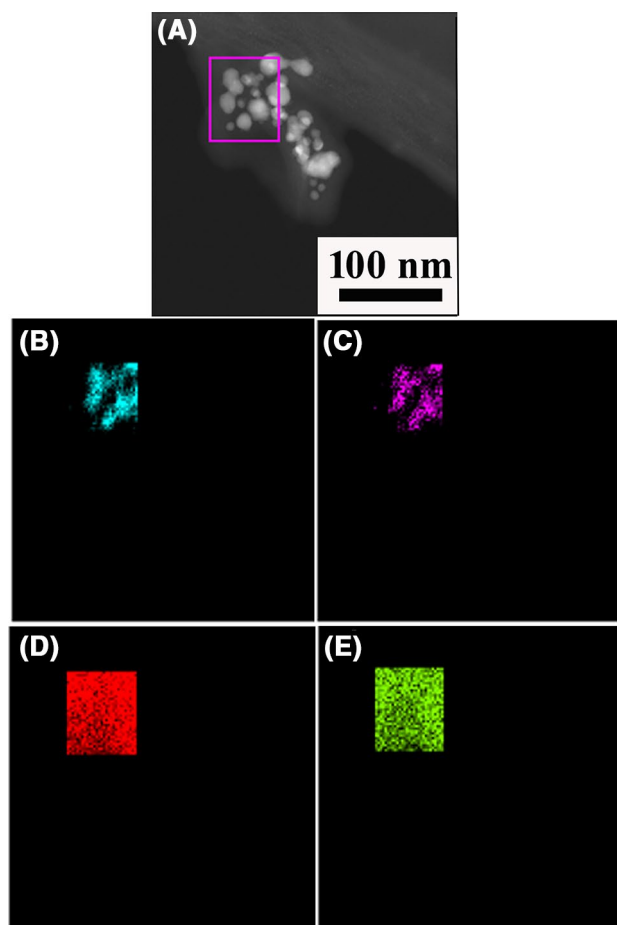


Fig. 2 TEM analysis of Ni–Co@C catalyst (Ni:Co=1:3): **a** TEM dark-field image; **b** elemental mapping of Co; **c** elemental mapping of Ni; **d** elemental mapping of C; **e** elemental mapping of O

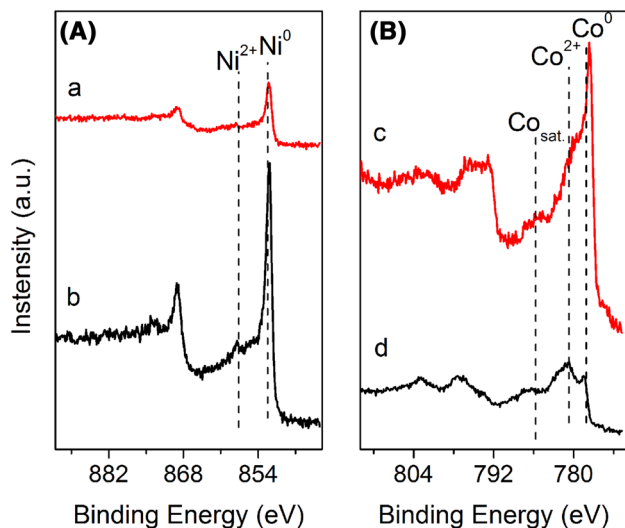


Fig. 3 **A** The Ni 2p XPS spectrum of Ni–Co@C (Ni:Co=1:3) (**a**) and Ni@C (**b**); **B** the Co 2p XPS spectrum of Ni–Co@C (Ni:Co=1:3) (**c**) and Co@C catalyst (**d**)

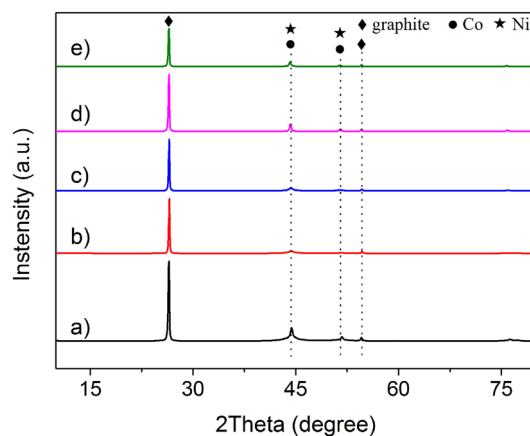
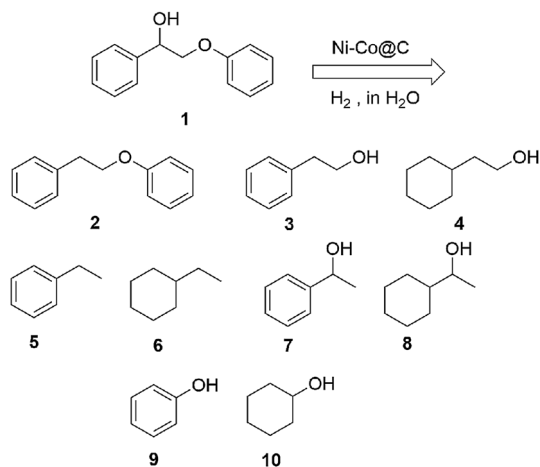


Fig. 4 XRD patterns of the Ni@C (**a**), Ni–Co@C (Ni:Co=1:1) (**b**), Ni–Co@C (Ni:Co=1:3) (**c**), Ni–Co@C (Ni:Co=1:5) (**d**) and Co@C (**e**)



Scheme 2 Product distribution of 2-phenoxy-1-phenylethanol hydro-treating over Ni–Co@C catalyst

cleavage are the main resulting compounds over nickel mono-metallic nanoparticles and no further hydrodeoxygenation takes place (Entry 8 in Table 1). Ni–Co bimetallic nanoparticles show tunable selectivity in the reaction routes with the change of the proportions of two metal species. Based on the experimental data in Table 1 and Fig. 5 reveals the trend about the catalytic selectivity of various Ni–Co bimetallic nanoparticles. It is noteworthy that the catalytic selectivity directly depends on the composition of bimetallic nanoparticles. Ni–Co@C (Ni:Co=1:3) catalyst shows the best performance with the hydrogenolysis selectivity of 83.7% with full conversion of substrate. Nickel species are active for ether bond cleavage and cobalt species work as hydrodeoxygenation catalysts. These two functions can be integrated to develop tunable catalytic selectivity for lignin hydrogenolysis.

Table 1 Screening experiments of hydrotreating 2-phenoxy-1-phenylethanol over various single-metal or bimetal catalysts coated with graphene layers

Entry	Catalysts	Conversion (%)	Selectivity (%)										Hydrogenolysis selectivity (%) ^a
			2	3	4	5	6	7	8	9	10		
1	Ni-Co@C (Ni:Co=1:1)	89.3	35.9	16.6	2.1	11.1	–	–	2.0	18.3	13.5	63.6	
2	Ni-Co@C (Ni:Co=1:2)	100	22.1	8.9	3.8	24.4	0.9	–	0.7	8.5	30.1	77.3	
3	Ni-Co@C (Ni:Co=1:3)	100	14.2	17.5	–	23.4	–	–	–	9.6	33.2	83.7	
4	Ni-Co@C (Ni:Co=1:4)	94.1	32.0	8.5	–	22.7	–	–	–	6.0	25.3	62.5	
5	Ni-Co@C (Ni:Co=1:5)	90.8	45.8	5.0	–	7.3	–	12.4	–	20.3	4.5	49.5	
6	Ni @C + Co@C (Ni:Co=1:3)	100	42.5	15.9	1.2	10.1	–	–	–	8.7	18.5	54.4	
7	Co@C	100	>99	–	–	–	–	–	–	–	–	0	
8	Ni @C	79.3	–	–	–	–	–	50	–	31.7	18.3	100	
9 ^b	Ni-Co@C (Ni:Co=1:3)	100	–	–	–	49	1	–	–	5.8	44.2	100	

Reaction condition: **1** (150 mg), catalyst (50 mg), EtOH (2 ml), H₂O (8 ml), H₂ (2 MPa), 170 °C/6 h

^aHydrogenolysis selectivity is the sum of products (**3+4+5+6+7+8+9+10**)

^bReaction condition: 2-phenylethyl phenyl ether **2** (150 mg), catalyst (50 mg), EtOH (2 ml), H₂O (8 ml), H₂ (2 MPa), 170 °C/6 h

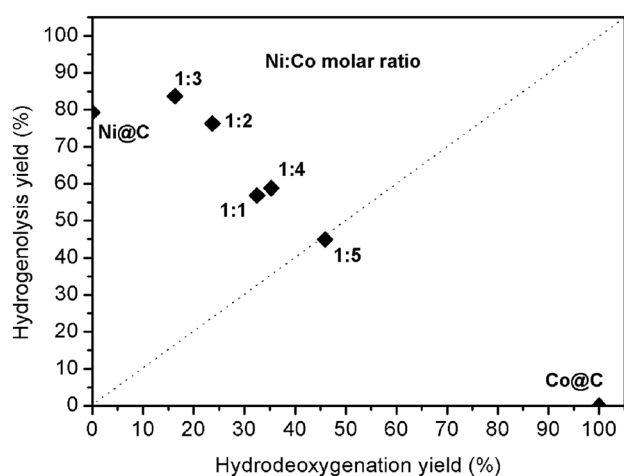


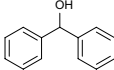
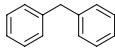
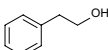
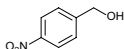
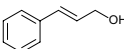
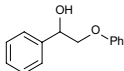
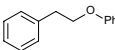
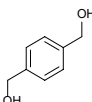
Fig. 5 The correlation between the reaction selectivity and the composition of bimetallic nanoparticles [hydrogenolysis yield is the sum of products (**3+4+5+6+7+8+9+10**) and hydrodeoxygenation yield is based on the product **2**]

Hydrodeoxygenation is a very important process to refine the product distribution during lignin hydrogenolysis. The catalytic performance of carbon-coated cobalt nanoparticles is further investigated in hydrodeoxygenation of various substrate molecules. As revealed in Entry 8 of Table 1, Co@C is a very efficient catalyst for hydrodeoxygenation. Its performances in catalytic conversion of other typical molecules are

summarized in Table 2. The reactions can proceed in a green solvent (H₂O/ethanol, 4:1) with high yield under relatively mild conditions. Benzyl alcohol, diphenyl-methanol, and 4-nitrobenzyl alcohol are totally converted to corresponding methylene compounds. Hydrogenolysis of 3-pyridinyl-methanol affords the 3-methylpyridine with a yield of 98.2%. The reaction of 1-phenylethanol and 1-(2-methoxyphenyl) ethanol give the target products in the yield of 98–99%. Cinnamyl alcohol is converted to allybenzene (yield: 91.8%) as the final product. However, the catalytic hydrogenolysis of cinnamyl alcohol over Pd/C only leads to the formation of *n*-propylbenzene [30]. Dehydroxylation of 2-phenylethanol only gave a moderate yield of ethylbenzene. The hydrogenolysis of 1, 4-phenylenedimethanol to *p*-tolylmethanol is completed after 12 h. 2-Phenoxy-1-phenylethanol was converted to phenylethoxy-benzene in excellent yield (>99%) under the optimal condition. Although Pd/C has been reported in the hydrogenolysis of 2-phenoxy-1-phenylethanol under high hydrogen pressure (5 MPa), the yield of phenylethoxybenzene was only 38% [31].

Ni-Co@C (Ni:Co=1:3) catalyst is also applied to catalyze hydrogenolysis of β -O-4 lignin-type dimmers (Table 3). These dimeric lignin model compounds are the analogous linkage units of lignin matrix as illustrated in Scheme 1. The substitute groups of phenyl rings make the lignin-type dimmers more active than 2-phenoxy-1-phenylethanol. Under the same reaction conditions, these dimeric lignin linkage

Table 2 Dehydroxylation of aromatic alcohols over Co@C catalyst

Entry	Substrates	Products	t (h)	Yield (%) ^[b]
1			6	>99
2			6	95.6
3			6	>99
4			6	>99
5			12	98.2
6			6	46.9
7			10	>99
8			10	91.8
9 ^[c]			6	>99
10			12	97.8

Reaction condition: alcohol (1 mmol), Co@C catalyst (50 mg, Co: 29.2 wt%), EtOH (2 ml), H₂O (8 ml), H₂ (2 MPa), 170 °C

^aYield determined by GC using anisole as an internal reference

^b150 °C/6 h

Table 3 Hydrogenolysis of dimeric lignin model compounds over Ni–Co@C (Ni:Co = 1:3) catalyst

Entry	Substituent groups	Conversion (%)	Hydrogenolysis selectivity (%)
1	R ₁ =OCH ₃ , R ₂ =OH	>99	90.1
2	R ₁ =H, R ₂ =OH	>99	87.3
3	R ₁ =H, R ₂ =OCH ₃	>99	89.5

Reaction condition: substrate (200 mg), catalyst (50 mg), EtOH (2 ml), H₂O (8 ml), H₂ (2 MPa), 170 °C/6 h

compounds can be converted totally and the hydrogenolysis selectivity values are all above 85%. These results reveal that Ni–Co@C (Ni:Co = 1:3) is a highly efficient catalyst for lignin depolymerization for producing value-added chemicals.

3.3 Magnetic Recyclability and Activity Stability

Another attractive point is the improved recyclability of Ni–Co@C (Ni:Co = 1:3) catalyst. Base metal (Ni, Co, Cu, Fe) hydrotreating catalysts generally show relatively poorer recyclability than noble metals. The graphene layers provide the protection against deactivation during recycling operation under the exposure to air and moisture. The magnetic properties of Ni–Co@C catalytic materials are beneficial to their separation from the reaction mixture. Figure 6 shows the magnetization curves of Co@C, Ni–Co@C (Ni:Co = 1:3), and Ni@C at room temperature. The hysteresis loops in

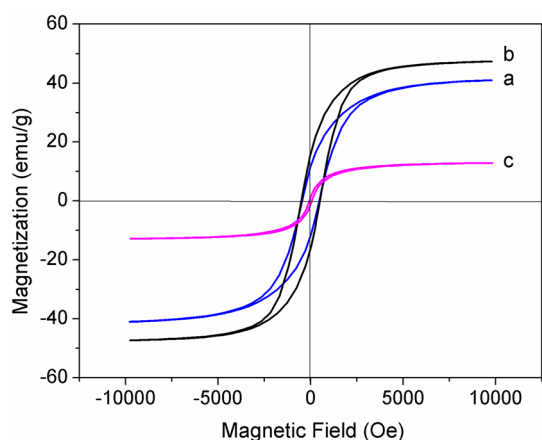


Fig. 6 Room temperature magnetization curves of *a* Co@C, *b* Ni-Co@C, *c* Ni@C

these catalysts confirmed their ferromagnetic behaviors. The corresponding saturation magnetization strengths (M_s) are 41.0 emu/g (Co@C), 47.3 emu/g (Ni-Co@C, Ni:Co = 1:3), and 12.9 emu/g (Ni@C). M_s values of these materials were much lower than those of the bulk cobalt (166 emu/g) [32] and nickel (51.3 emu/g) [33]. This is mainly attributed to size effects of metal nanoparticles and the presence of carbon layers. However, the M_s value of Ni-Co@C affords a proper ferromagnetic parameter for the efficient magnetic separation. After the reaction, Ni-Co@C catalysts are readily separated from the liquid mixtures by magnet with high recycling ratio. The catalyst is input into the next batch reaction after simple washing treatment.

As revealed in Fig. 7a, a 12-run recycling test is carried out to investigate the recyclability and recoverability of Ni-Co@C (Ni:Co = 1:3) during batch-by-batch hydrogenolysis of 2-phenoxy-1-phenylethanol. After the ninth testing run, there is a tendency toward deactivation. The vanishment of protection of carbon coating has directly led to oxidation of active metallic species. During the practical operation, it is inevitable that carbon layers over bimetallic nanoparticles are gradually worn away by the intergranular friction, the collision with the stirrer and autoclave wall, and the leaching effect of the solvent. TEM image of the Ni-Co@C after the sixth run shows that some abrasion and dislocation of carbon layers are observed (Fig. 7b). Further recycling test leads to the gradual loss of carbon layers. They vanish after the tenth run and the deactivation is observed. However, the loss of catalytic activity shows little impact on the catalytic selectivity. It is clearly revealed that graphene protection layers play a key role in improving catalytic stability of the bimetallic nanoparticles.

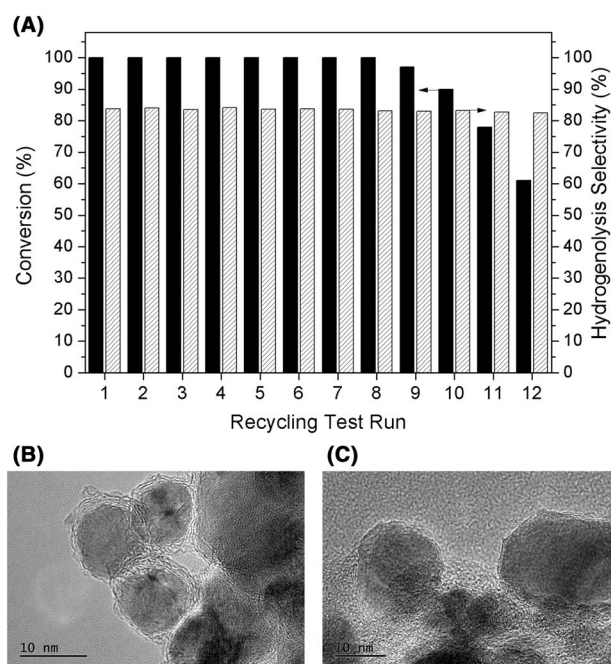


Fig. 7 **a** 12-run recycling test of Ni-Co@C (Ni:Co = 1:3) catalyst. **b** TEM image of the catalyst after the sixth recycling run. **c** TEM image of the catalyst after the tenth recycling run

4 Conclusion

In summary, nickel-cobalt mixed nanoparticles, coated with several layers of graphene, were prepared by the modified Pechini-type sol-gel method and the following controlled heating treatment. This nanocatalysts showed unexpectedly tunable selectivity in catalytic hydrotreating of model molecule of phenylpropane linkages in lignin. Dimeric lignin model compounds can be converted totally and the hydrogenolysis selectivities were above 85%. The catalytic selectivity directly depends on the composition of bimetallic nanoparticles. The recyclability and recoverability of Ni-Co@C (Ni:Co = 1:3) was investigated through a 12-run recycling test. The deposition of graphene layers over the metal nanoparticles markedly improves their stability to air and moisture. The nanocatalyst showed excellent recyclability and can be reused ten times without significant loss of activity.

Acknowledgements This work was financially supported by the National Natural Sciences Foundation of China (Nos. 21403248, 21174148, 21101161).

References

- Li CZ, Zhao XC, Wang AQ, Huber GW, Zhang T (2015) Chem Rev 115:11559–11624
- Zaheer M, Kempe R (2015) ACS Catal 5:1675–1684

3. Sturgeon MR, Kim S, Lawrence K, Paton RS, Chmely SC, Nimlos M, Foust TD, Beckham GT (2014) *ACS Sustain Chem Eng* 2:472–485
4. Holladay JE, White JF, Bozell JJ, Johnson D (2007) Top Value-added chemicals from biomass. Vol. II-results of screening for potential candidates from biorefinery lignin. Pacific Northwest National Laboratory, Richland, WA, p PNNL-16983
5. Vanholme R, Demedts B, Morreel K, Ralph J, Boerjan W (2010) *Plant Physiol* 153:895–905
6. Bjorsvk HR, Liguori L (2002) *Org Process Res Dev* 6:279–290
7. Bozell JJ (2014) *Top Curr Chem* 353:229–255
8. Pandey A, Bhaskar T, Stocker M, Sukumaran R (2015) Recent advances in thermochemical conversion of biomass. Elsevier, Waltham
9. Strassberger Z, Alberts AH, Louwerse MJ, Tanase S, Rothenberg G (2013) *Green Chem* 15:768–774
10. Chen MY, Huang YB, Pang H, Liu XX, Fu Y (2015) *Green Chem* 17:1710–1717
11. Zhou XY, Mitra J, Rauchfuss TB (2014) *ChemSusChem* 7:1623–1626
12. Galkin MV, Sawadjoon S, Rohde V, Dawange M, Samec JSM (2014) *ChemCatChem* 6:179–184
13. Kim JK, Lee JK, Kang KH, Lee JW, Song IK (2015) *J Mol Catal A* 410:184–192
14. Zhang JG, Asakura H, van Rijn J, Yang J, Duchesne P, Zhang B, Chen X, Zhang P, Saeys M, Yan N (2014) *Green Chem* 16:2432–2437
15. Zhang JG, Teo J, Chen X, Asakura H, Tanaka T, Teramura K, Yan N (2014) *ACS Catal* 4:1574–1583
16. He JY, Zhao C, Lercher JA (2012) *J Am Chem Soc* 134:20768–20775
17. Molinari V, Giordano C, Antonietti M, Esposito D (2014) *J Am Chem Soc* 136:1758–1761
18. Sturgeon MR, O'Brien MH, Ciesielski PN, Katahira R, Kruger JS, Chmely SC, Hamlin J, Lawrence K, Hunsinger GB, Foust TD, Baldwin RM, Bidy MJ, Beckham GT (2014) *Green Chem* 16:824–835
19. Cui XJ, Yuan HK, Junge K, Topf C, Beller M, Shi F (2017) *Green Chem* 19:305–310
20. Cole-Hamilton DJ (2003) *Science* 299:1702–1706
21. Corma A, Garcia H, Xamena FXL (2010) *Chem Rev* 110:4606–4655
22. Ogasawara S, Kato S (2010) *J Am Chem Soc* 132:4608–4613
23. Schoemaker HE, Mink D, Wubbolts MG (2003) *Science* 299:1694–1697
24. Friedfield MR (2013) *Science* 342:1076–1080
25. Galyis HMT (2012) *Science* 335:835–838
26. Westerhaus FA, Jagadeesh RV, Wienhofer G, Pohl MM, Radnik J, Surkus AE, Rabeah J, Junge K, Junge H, Nielsen M, Bruckner A, Beller M (2013) *Nat Chem* 5:537–543
27. Calderone VR, Shiju NR, Curulla-Ferr D, Chambrey S, Khodakov A, Rose A, Thiessen J, Jess A, Rothenberg G (2013) *Angew Chem Int Ed* 52:4397–4401
28. Smith RDL, Prévot MS, Fagan RD, Trudel S, Berlinguette CP (2013) *J Am Chem Soc* 135:11580–11586
29. Chen B, Li F, Huang Z, Yuan G (2017) *Appl Catal B* 200:192–199
30. Mirza-Aghayan M, Tavana MM, Boukherroub R (2015) *Catal Commun* 69:97–103
31. Galkin MV, Dahlstrand C, Samec JSM (2015) *ChemSusChem* 8:2187–2192
32. Tan CG, Grass RN (2008) *Chem Commun* 36:4297–4299
33. Si PZ, Zhang ZD, Geng DY, You CY, Zhao XG, Zhang WS (2003) *Carbon* 41:247–251